

Supporting Information for

Mixture is Better: Enhanced Electrochemical Performance of Phenyl Selenosulfide in Rechargeable Lithium Batteries

By *Wei Guo, Amruth Bhargav, Joseph D. Ackerson, Yi Cui, Ying Ma,* and Yongzhu Fu**

Experimental Section:

Materials: Lithium bis(trifluoromethanesulfonimide) (LiTFSI, $\text{LiN}(\text{CF}_3\text{SO}_2)_2$, 99%, Acros Organics), lithium nitrate (LiNO_3 , 99.999%, Acros Organics), 1,2-dimethoxyethane (DME, 99.5%, Sigma Aldrich), 1,3-dioxolane (DOL, 99.8%, Sigma Aldrich), phenyl disulfide (PhS-SPh, $\text{C}_6\text{H}_5\text{SSC}_6\text{H}_5$, 99%, Sigma Aldrich), and phenyl diselenide (PhSe-SePh, $\text{C}_6\text{H}_5\text{SeSeC}_6\text{H}_5$, 99%, Acros Organics) were purchased and used as received.

Synthesis of phenyl selenosulfide (PhS-SePh): Equimolar PhS-SPh and PhSe-SePh were mixed in DME solvent. The solution was stirred for 2 h and DME was removed by evaporation. The product was obtained for further analysis.

Electrolyte and catholyte preparation: The electrolyte is composed of 1.0 M LiTFSI and 0.1 M LiNO_3 in mixture solvent of DME and DOL (1:1 v/v). 0.5 M or 1.0 M catholytes were prepared by adding appropriate amounts of active materials (PhS-SPh, PhSe-SePh, or PhS-SePh) to the electrolyte. The electrolyte and catholytes were prepared and stored in an Argon-filled glove box.

Li cell fabrication and electrochemical evaluation: Commercial binder-free carbon nanotube paper called buckypaper (NanoTechLabs, Inc) was used as the current collector in this study. The carbon paper was cut into 0.97 cm² discs ($D = 11$ mm, about 2 mg each) and dried at 100 °C for 24 h in a vacuum oven before use. Coin cells CR2032 were fabricated in the glove box. First, catholyte (20 μL) was added into the buckypaper current collector. Then a Celgard 2400 separator was placed on the top of the electrode followed by adding 20 μL blank electrolyte on the top of the separator. Finally, lithium metal anode was placed on the separator. The cell was crimped and taken out of the glove box for testing.

Cyclic voltammetry (CV) was performed on a BioLogic VSP potentiostat. The potential was swept from open circuit voltage to 1.8 V and then swept back to 2.8 V at a scanning rate of 0.02 mV s⁻¹. Cells were galvanostatically cycled between 1.8 and 2.8 V on an Arbin BT2000 battery cycler at different C rates (1C = 245.5 mA g⁻¹ for PhS-SPh, 1C = 171.7 mA g⁻¹ for PhSe-SePh, and 1C = 202.1 mA g⁻¹ for PhS-SePh, based on their masses in the cells).

Characterizations:

The X-ray diffraction (XRD) data were collected on a Bruker D8 Discover XRD Instrument equipped with Cu K α radiation. The scanning rate was 2° min⁻¹, and 2 θ was set between 10° and 60°. The morphological characterization of the discharged electrodes was conducted with a JEOL JSM-7800F field emission scanning electron microscopy (SEM).

Fourier transform infrared (FTIR) absorption spectra were recorded on a Thermo Scientific-Nicolet iS10 FTIR spectrometer. 64 scans between 400 cm^{-1} to 485 cm^{-1} were recorded per sample. Samples were prepared by grinding the compounds with KBr and pelletizing it using an FTIR die set.

GC-MS were analyzed with an Agilent 7890A gas chromatograph coupled to an Agilent 5975C mass spectrometer. The column is an Agilent J&W HP-5ms Ultra Inert GC Column, with the following specifications: 30 m column length, 0.25 mm internal diameter, 0.25 μm film thickness. The inlet was held at $250\text{ }^\circ\text{C}$ with a split flow of 1.024 mL /min (He carrier gas). 0.1 M solution of the samples was placed inside a 3 mL testing vial, then $1\text{ }\mu\text{L}$ solution was injected into the GC machine with microneedle with a split ratio of 50:1. The oven temperature program utilized an initial temperature of $80\text{ }^\circ\text{C}$ held for 3 minutes, followed by a ramp of $10\text{ }^\circ\text{C min}^{-1}$ to $280\text{ }^\circ\text{C}$. The MS transfer line temperature was $250\text{ }^\circ\text{C}$. The mass spectrometer utilized an electron impact detector with a 3 min solvent delay and a scan range of $m/z = 26\text{-}320$. The relevant components of each sample were identified based on the mass spectra in the National Institute of Standards and Technology (NIST) version 08 mass spectral database.

^{13}C -NMR spectra were collected using a Bruker Avance III 500 MHz NMR spectrometer. The 0.1 M solution of the material of interest was prepared in CDCl_3 . $700\text{ }\mu\text{L}$ of the solution was subject to NMR analysis and the chemical shifts (δ) are referenced downfield from tetramethylsilane (TMS, $(\text{CH}_3)_4\text{Si}$) using the residual solvent peak as an internal standard.

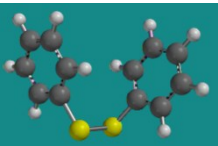
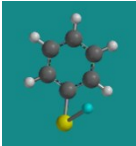
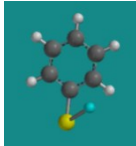
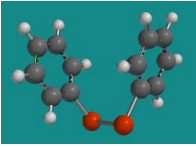
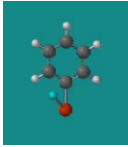
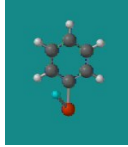
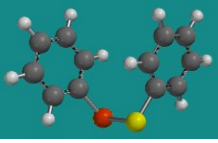
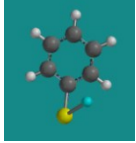
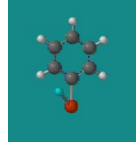
Simulation: For crystal structure determination, first-principles structural optimization based on the density function theory (DFT) was performed using the projector augmented wave method¹ as implemented in the Vienna Atomistic Simulation Package (VASP).²⁻³ The exchange correlation potential was described by a generalized gradient approximation with the Perdew-Burke-Ernzerhof parameterization.⁴ The structures were relaxed until the force on each atom was less than 0.02 eV/\AA .

First-principles DFT calculations were performed using SPARTAN software package (Wave function, Irvine, CA) to determine the equilibrium geometry and energetics of various molecules studied in this work. The M06-2X exchange-correlation functional and the 6-31G* basis set were used. To simulate the effect of the catholyte solution, a polarizable continuum model (PCM) was used, and the dielectric constant was set to that of DME that was used as the electrolyte in this study (the dielectric constant of DOL is similar to that of DME).

Table S1. The crystal structures have been optimized computationally, and the optimized structures are given below. Data for PhS-SPh and PhSe-SePh are obtained from literature.⁵

	PhS-SPh	PhSe-SePh	PhS-SePh
a	5.230 (5.540)	5.307 (5.570)	5.245
b	7.818 (8.086)	7.952 (8.238)	7.888
c	22.924 (23.478)	23.450 (23.826)	23.125

Table S2. Calculation of energy changes of lithiation reactions of PhS-SPh, PhSe-SePh, and PhS-SePh.

PhS-SPh	2Li	→	PhS-Li	PhS-Li
 <p>PhS-SPh Energy: -1259.41182 au E HOMO: -7.77 eV E LUMO: -0.69 eV Middle Bond: 2.0151 eV</p>	2Li		 <p>PhSLi Energy: -637.283037 au E HOMO: -6.74 eV E LUMO: -0.36 eV</p>	 <p>PhSLi Energy: -637.283037 au E HOMO: -6.74 eV E LUMO: -0.36 eV</p>
Total Energy: -1259.41182 au			Total Energy: -1274.566074 au	
PhSe-SePh	2Li	→	PhSe-Li	PhSe-Li
 <p>PhSe-SePh Energy: -5265.66721 au E HOMO: -7.53 eV E LUMO: -0.99 eV Middle Bond: 1.6972 eV</p>	2Li		 <p>PhSeLi Energy: -2640.40751 au E HOMO: -6.67 eV E LUMO: -0.36 eV</p>	 <p>PhSeLi Energy: -2640.40751 au E HOMO: -6.67 eV E LUMO: -0.36 eV</p>
Total Energy: -5265.66721 au			Total Energy: -5280.81502 au	
Ph-S-Se-Ph	2Li	→	Ph-S-Li	Ph-Se-Li
 <p>PhS-SePh Energy: -3262.53928 au E HOMO: -7.64 eV E LUMO: -0.86 eV Middle Bond: 1.8498 eV</p>	2Li		 <p>PhSLi Energy: -637.283037 au E HOMO: -6.74 eV E LUMO: -0.36 eV</p>	 <p>PhSeLi Energy: -2640.40751 au E HOMO: -6.67 eV E LUMO: -0.36 eV</p>
Total Energy: -3262.53928 au			Total Energy: -3277.690547 au	

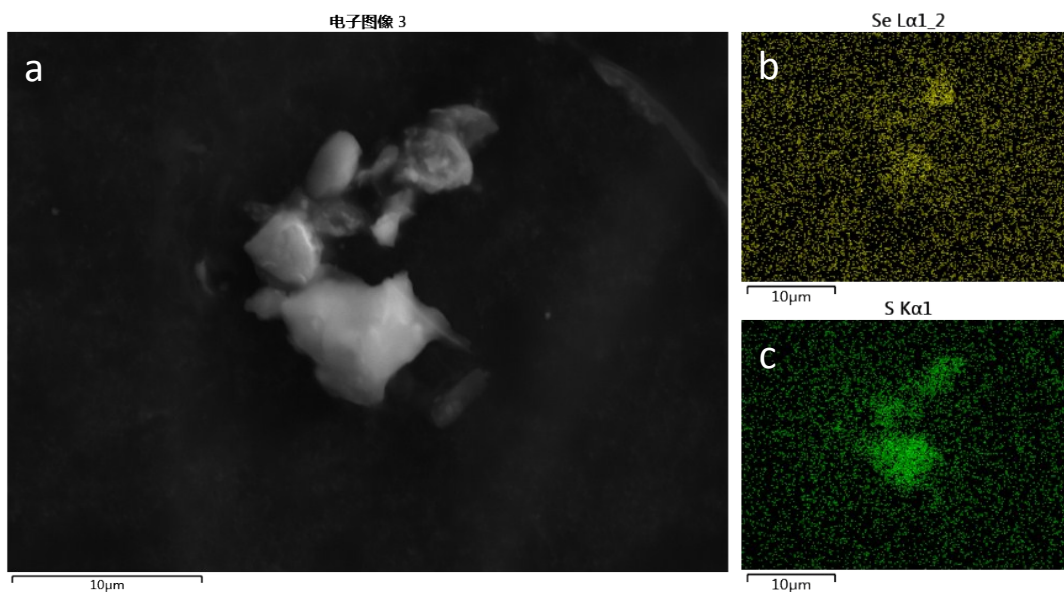


Figure S1. Scanning electron microscopy image (a), selenium mapping (b), and sulfur mapping (c) of PhS-SePh. The Se and S atomic ratios are almost the same in the as-prepared sample.

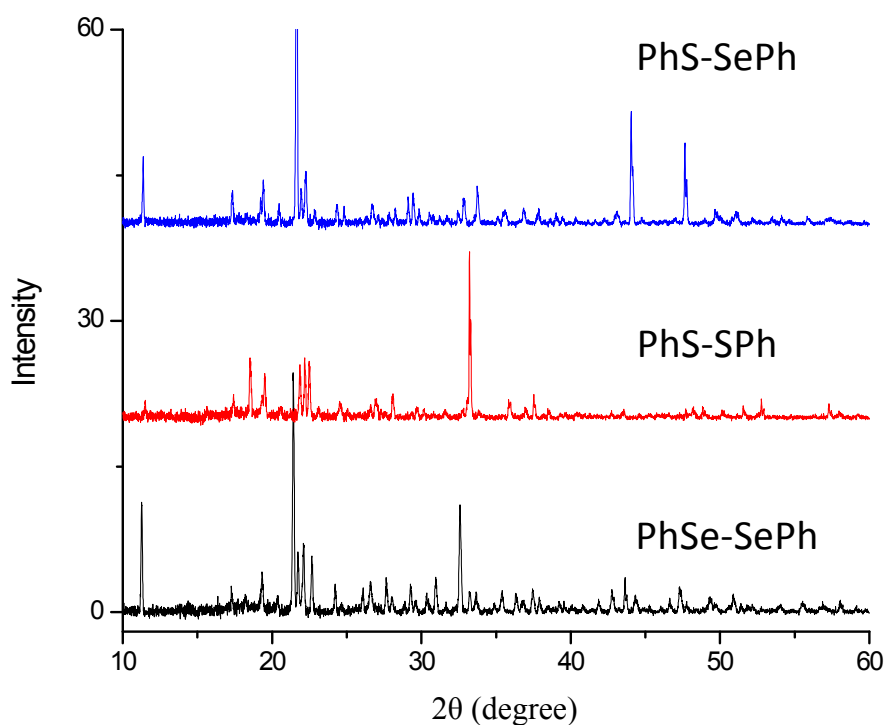


Figure S2. X-ray diffraction patterns of PhS-SPh, PhSe-SePh, and PhS-SePh.

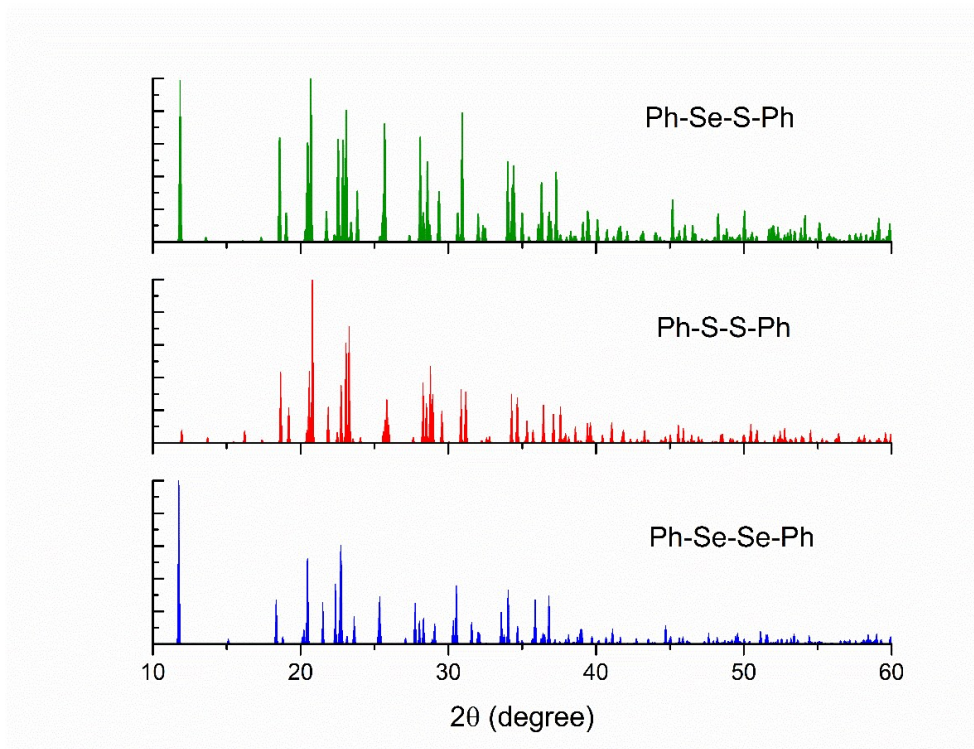


Figure S3. Calculated X-ray diffraction patterns of PhS-SPh, PhSe-SePh, and PhS-SePh.

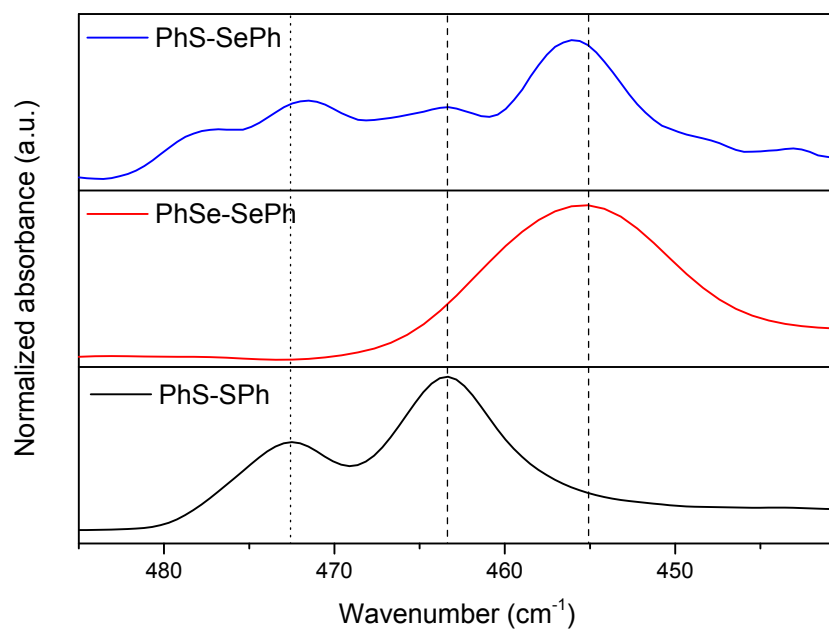


Figure S4. FTIR spectra of PhS-SPh, PhSe-SePh, and PhS-SePh. The dashed lines represent the out of plane phenyl ring deformation. The dotted line represents the S-S bond stretch.

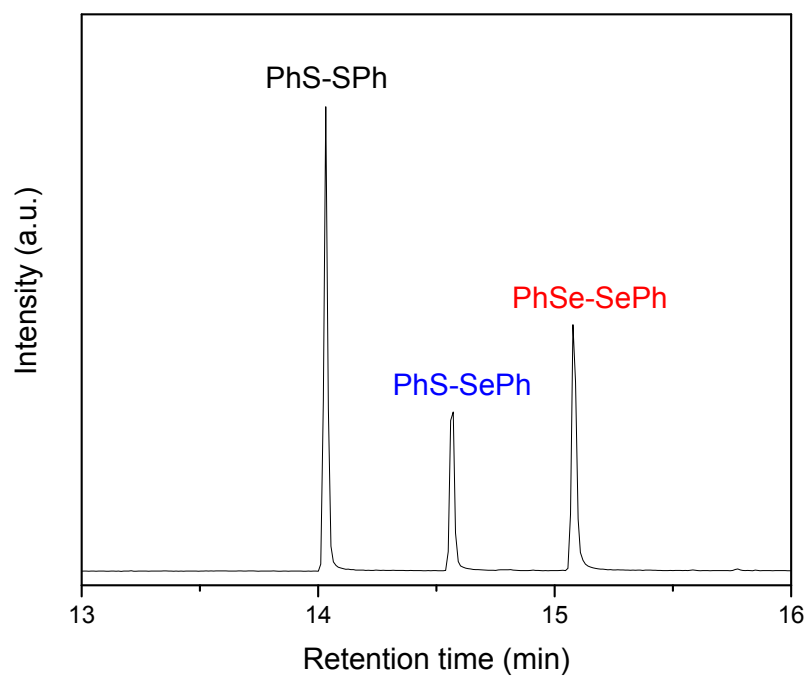


Figure S5. Gas chromatograph of PhS-SePh sample.

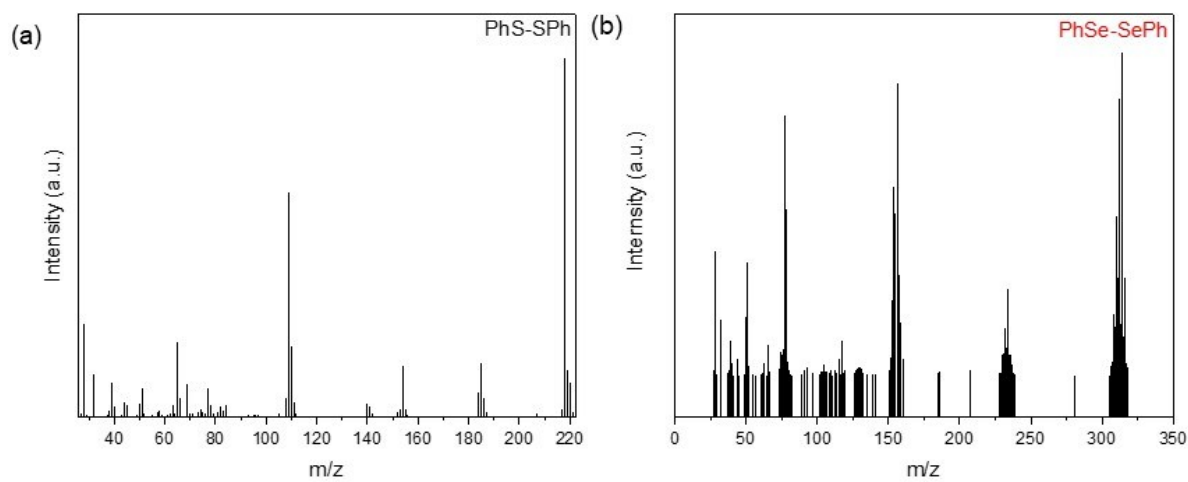


Figure S6. Mass spectra of PhS-SePh at 14.1 (a) and 15.1 min (b).

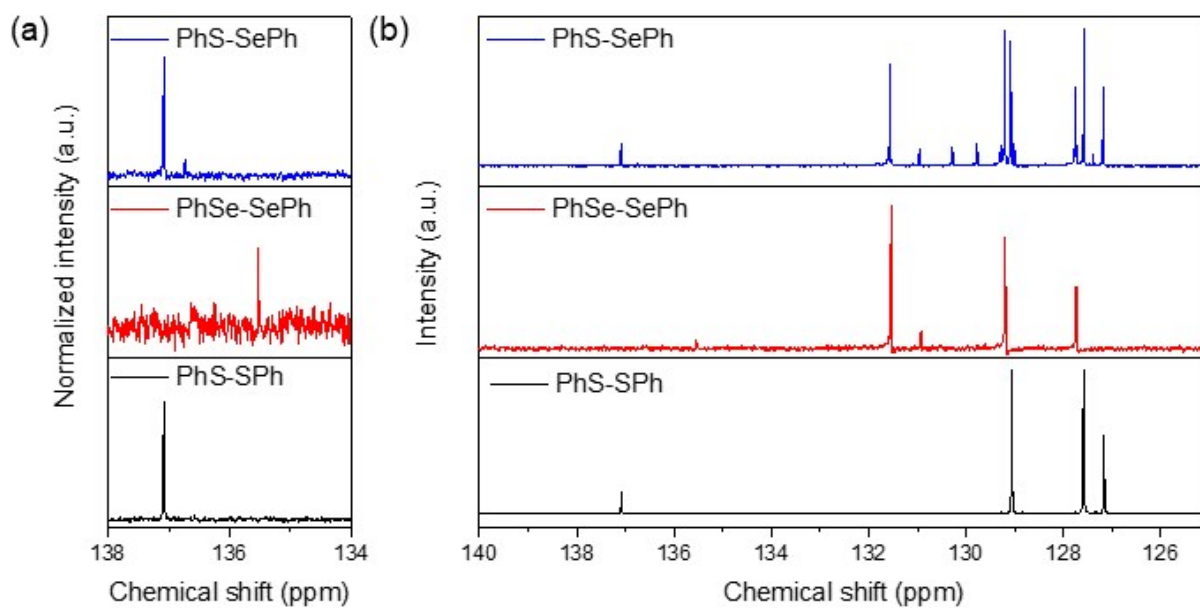


Figure S7. ^{13}C -NMR spectra of PhS-SPh, PhSe-SePh, and PhS-SePh showing (a) the quaternary carbon region and (b) the full spectrum.

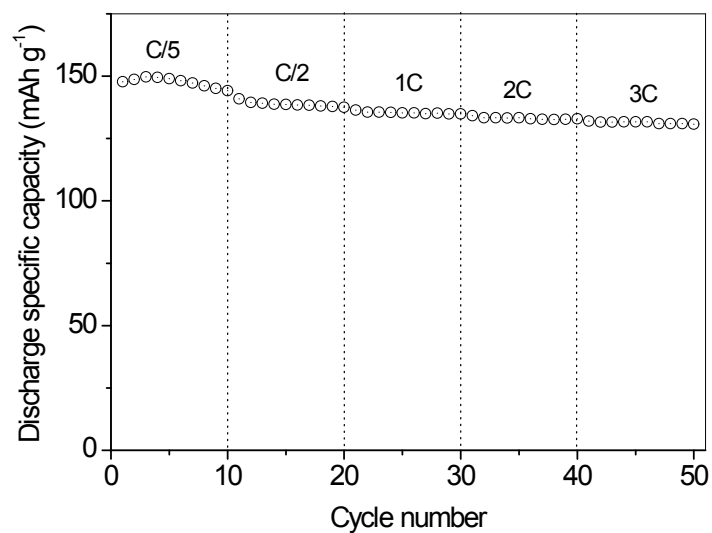


Figure S8. The cell with 0.5 M PhS-SePh catholyte at different C rates.

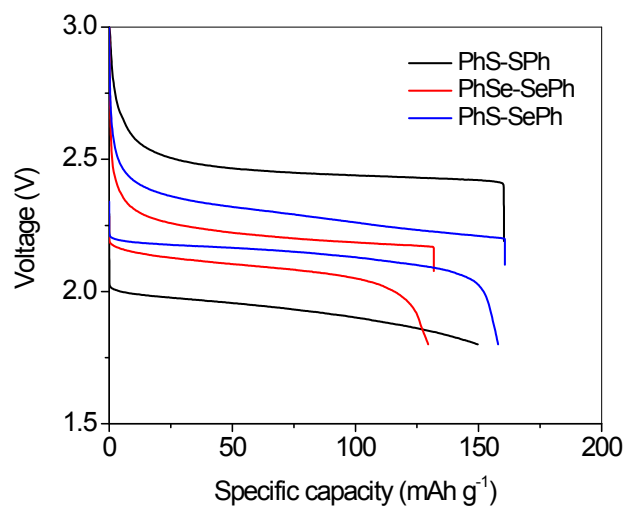


Figure S9. Voltage profiles of cells with 1.0 M PhS-SPh, PhSe-SePh, and PhS-SePh catholytes at $C/5$.

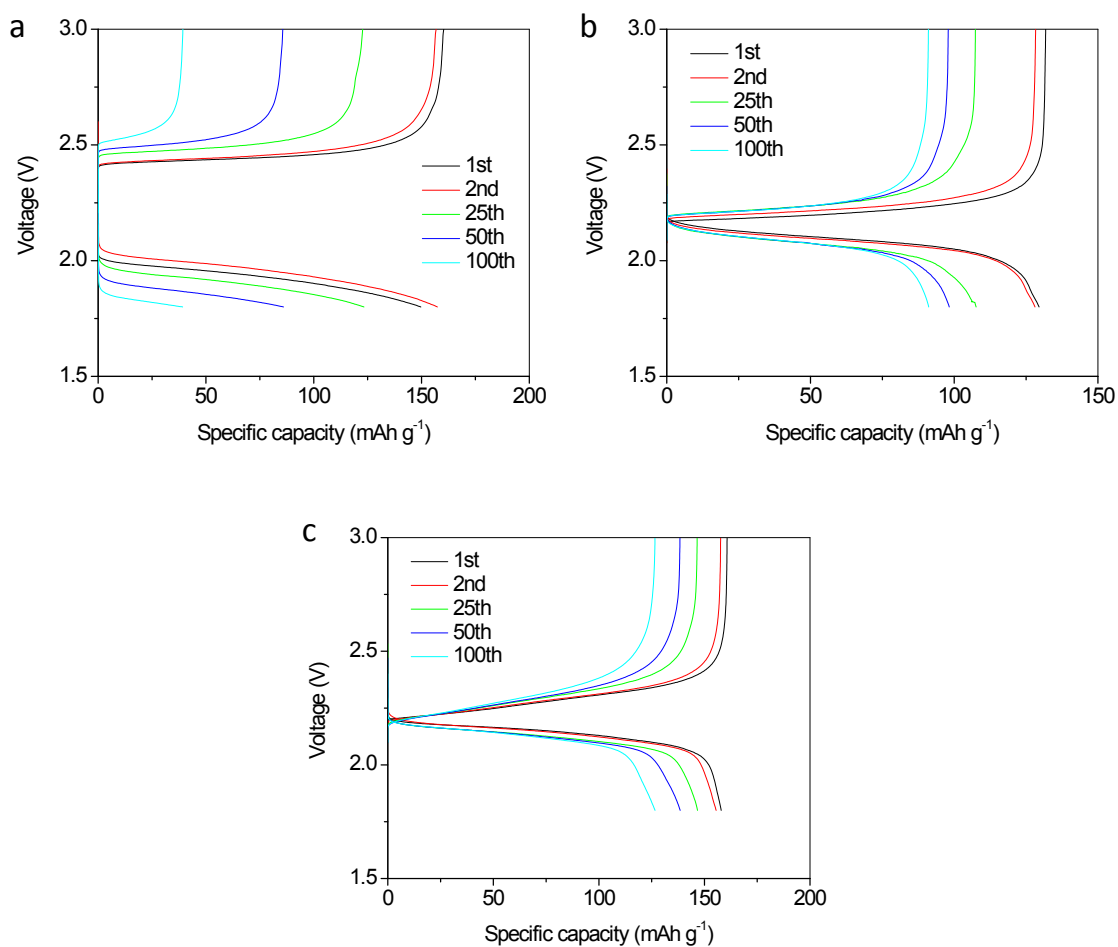


Figure S10. Selected voltage profiles of cells with 1.0 M PhS-SPh (a), PhSe-SePh (b), and PhS-SePh (c) catholytes at $C/5$.

1. Blochl, P. E., Projector Augmented-Wave Method. *Phys. Rev. B* **1994**, *50*, 17953-17979.
2. Kresse, G.; Furthmuller, J., Efficiency of ab-initio total energy calculation for metals and semiconductors using plane wave basis set. *Comput. Mat. Sci.* **1996**, *6*, 15-50.
3. Kresse, G.; Furthmuller, J., Efficient iterative schemes for ab-initio total energy calculations using a plane-wave basis set. *Phys. Rev. B* **1996**, *54*, 11169-11186.
4. Perdew, J. P.; Burke, K.; Ernzerhof, M., Generalized Gradient Approximation Made Simple. *Phys. Rev. Lett.* **1996**, *77*, 3865.
5. A. L. Fuller, L. A.S. Scott-Hayward, Y. Li, M. Buhl, A. M.Z. Slawin and J. D. Woollins, Automated Chemical Crystallography. *J. Am. Chem. Soc.* **2010**, *132*, 5799-5802.